UNIVERSITÉ DE GENÈVE

Archive ouverte UNIGE
https://archive-ouverte.unige.ch

Article scientifique | Article | 1997

Published version | Open Access

This is the published version of the publication, made available in accordance with the publisher's policy.

Age of Cu(-Fe)-Au mineralization and thermal evolution of the Punta del Cobre district, Chile

Marschik, Robert; Singer, B. S.; Munizaga, F.; Tassinari, C.; Moritz, Robert; Fontboté, Lluís

How to cite

MARSCHIK, Robert et al. Age of Cu(-Fe)-Au mineralization and thermal evolution of the Punta del Cobre district, Chile. In: Mineralium deposita, 1997, vol. 32, n° 6, p. 531–546. doi: 10.1007/s001260050120

This publication URL: https://archive-ouverte.unige.ch/unige:27824
Publication DOI: 10.1007/s001260050120

© This document is protected by copyright. Please refer to copyright holder(s) for terms of use.

Mineralium Deposita (1997) 32: 531–546 © Springer-Verlag 1997

ARTICLE

R. Marschik · B.S. Singer · F. Munizaga · C. Tassinari
R. Moritz · L. Fontboté

Age of Cu(-Fe)-Au mineralization and thermal evolution of the Punta del Cobre district, Chile

Received: 2 July 1996 / Accepted: 11 March 1997

Abstract The Punta del Cobre belt is located 15 km south of Copiapó, northern Chile. It comprises several Cu(-Fe)-Au deposits in the Punta del Cobre and Ladrillos districts, east of the Copiapó river, and the Ojancos Nuevo district, with the new Candelaria mine, and Las Pintadas district, west of the river. The mineralization in the Punta del Cobre belt is characterized by a simple hypogene mineral assemblage of chalcopyrite, pyrite, magnetite, and hematite. Average ore grades are 1.1 to 2% Cu, 0.2 to 0.6 g/t Au, and 2 to 8 g/t Ag. Massive magnetite occurs as veins and irregularly shaped bodies. The ore is spatially associated with alkali metasomatism and in particular with potassic alteration. The Cu(-Fe)-Au deposits are hosted mainly in volcanic rocks of the Punta del Cobre Formation (pre-upper Valanginian) that underlie Neocomian limestones of the Chañarcillo Group. This region experienced backarc basin formation in the Neocomian, uplift and granitoid intrusions in the middle Cretaceous, and eastward migration of the magmatic front of about 30 km between middle Cretaceous and Paleocene. To determine the timing of ore deposition and to reconstruct parts of the thermal history of the Punta del Cobre district, in the eastern part of the belt, we have obtained $^{40}Ar/^{39}Ar$ incremental-heating and Rb-Sr analyses of mineral and whole-rock samples. An $^{40}Ar/^{39}Ar$ incremental-heating experiment on hydrothermal biotite, formed synchronous with the Cu(-Fe)-Au mineralization, yielded an inverse isochron age of 114.9 ± 1.0 Ma (all errors reported at $\pm 2\sigma$), consistent with a Rb-Sr isochron of 116.8 ± 2.7 Ma calculated from 7 whole-rock samples. These data are interpreted to represent the age of potassic alteration that accompanies mineralization. Ore formation temperatures of 400 °C to 500 °C were previously estimated based on paragenetic relationships. Shearing at the Candelaria deposit occurred after ore deposition and before the main stage of batholith emplacement. Published K-Ar ages for the middle Cretaceous batholith near the Punta del Cobre belt range from 119 to 97 Ma. Our data suggest that the mineralization is related to the earlier stages of batholith emplacement. The biotite age spectrum indicates that the Punta del Cobre district was not affected by temperatures above ~300 °C–350 °C, the closure temperature for argon in biotite, during the contact metamorphic overprint produced by later emplaced batholithic intrusions. Whole-rock $^{40}Ar/^{39}Ar$ ages are considerably younger; incremental-heating experiments yielded an inverse isochron age of 90.7 ± 1.2 Ma and weighted mean plateau ages of 89.8 ± 0.6 Ma and 89.5 ± 0.6 Ma. These samples are dominantly K-feldspar, for which we assume an argon closure temperature of ~150 °C, thus they give the age of cooling below ~150 °C–200 °C.

Editorial handling: DR

R. Marschik[1] (✉) · B.S. Singer (✉) · R. Moritz · L. Fontboté
Département de Minéralogie, Université de Genève,
Rue des Maraîchers 13, 1211 Genève 4, Switzerland

F. Munizaga
Departamento de Geología y Geofísica, Universidad de Chile,
Casilla 13518 Correo 21, Santiago, Chile

C. Tassinari
Instituo de Geociências, Universidade de São Paulo,
Caixa Postal 20899, São Paulo, Brazil

Present address:
[1]Departamento de Geología, C.C. Minera Candelaria,
Tierra Amarilla, Chile

Introduction

The Punta del Cobre belt is located in the Atacama region near the city of Copiapó (Fig. 1). The belt comprises several Cu(-Fe)-Au deposits in the Punta del Cobre (e.g., Carola, Resguardo, Santos, Socavón Rampa, and Trinidad mines) and southern Ladrillos districts (Mantos de Cobre mine), east of the Copiapó river. West of the Copiapó river are located the new Candelaria deposit (366 Mt of 1.08% Cu and 0.26 g/t Au) in the Ojancos Nuevo district, and some smaller

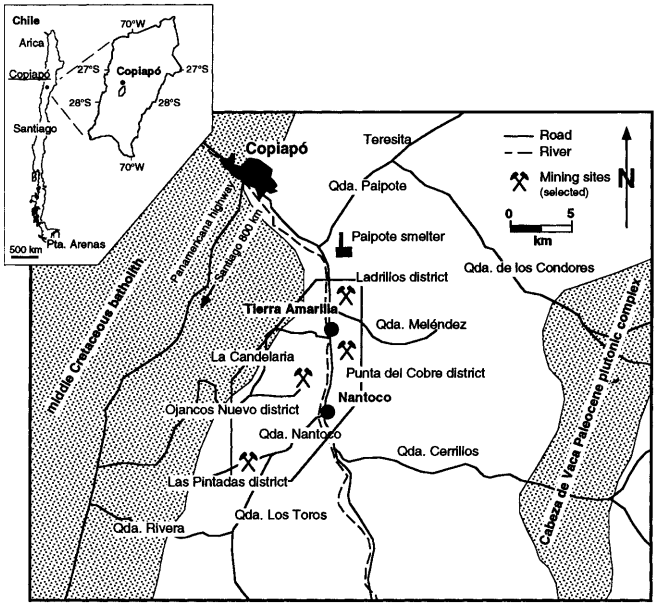

Fig. 1 Location of the studied part of the Punta del Cobre belt. The position of major intrusive complexes is indicated

mines in the Las Pintadas district (e.g., Farola-Las Pintadas, Abandonada, Resguardo; Fig. 2). There has been mining activity in the area at least since the seventeenth century. Modern mining commenced in 1929 and was reinforced in 1952 as the Planta Aguirre Cerda mill and the Paipote smelter, respectively, went into production (Segerstrom and Ruiz 1962). After the discovery of the Candelaria orebodies in 1987 the area again became an active exploration target. With startup of the new Candelaria mine and positive exploration results, the Punta del Cobre belt is of increasing economic importance for Chile's mineral production.

The determination of mineralization ages is critical in the understanding of ore forming processes and the development of conceptual models that are the basis for successful exploration. Direct dating of ore is only occasionally possible because of the lack of suitable minerals (e.g., York et al. 1981; Nakei et al. 1993; Brannon et al. 1992; Chesley et al. 1994). Indirect dating based on isotopic age determinations of cogenetic alteration and gangue minerals is, however, a widely used tool to constrain the time of the ore deposition (e.g., Sutter et al. 1983; Snee et al. 1988; Perkins 1996).

This contribution is the first to present age determinations of alteration related to mineralization in the Punta del Cobre belt. A description and discussion of the alteration and possible genetic models is given in Marschik and Fontboté (1996). The present work reports age determinations using whole-rock samples and mineral separates from the Punta del Cobre district using $^{40}Ar/^{39}Ar$, Rb-Sr, and K-Ar techniques. Cooling ages combined with temperature estimates based on fluid inclusions in post-ore calcite and the chlorite thermometer of Cathelineau and Nieva (1985) allow us to constrain parts of the thermal and metasomatic history of the Punta del Cobre and southern Ladrillos districts.

Geological setting

The mainly volcanic Punta del Cobre Formation hosts the Cu(-Fe)-Au mineralization of the Punta del Cobre belt. These rocks underlie upper Valanginian to Aptian shallow marine carbonate sediments of the Chañarcillo Group (Abundancia, Nantoco, Totoralillo, and Pabellón Formations) that were deposited in the Andean backarc basin. After uplift of the area above sea level in the middle Cretaceous, the lens-shaped volcanic and volcaniclastic Cerrillos Formation, which reaches a thickness of 4500 m, was unconformably deposited on the partly eroded rocks of the Chañarcillo Group (Segerstrom and Parker 1959; Jurgan 1977). The interplay of further continental deposition and denudation resulted in four episodes of landscape evolution (Sillitoe et al. 1968; Mortimer 1973). By middle Tertiary the erosion level was close to the recent surface. Large parts of the Atacama region were covered by alluvial deposits of Miocene age, the Atacama Gravels, which are well preserved as gravel terraces in the Punta del Cobre area (Segerstrom 1967; Mortimer 1973).

In the Punta del Cobre and Ladrillos districts, east of the Copiapó river, the Punta del Cobre Formation consists of a lower, hydrothermally altered, volcanic unit comprising the andesitic Lavas Inferiores and the "Albitófiro". The "Albitófiro" is an originally dacitic volcanic rock, which suffered strong albitization and, in places, is also affected by potassic alteration. Sediments that include breccias (Basal Breccia), and siltstone, chert, and limestone (Trinidad Member) rest unconformably above the "Albitófiro" (Fig. 2). These sediments record a transition from terrestrial to shallow marine environments. The Trinidad Member is overlain by the Lavas Superiores consisting of lava flows, volcanic breccias, and tuffs. The Lavas Superiores represent the uppermost member of the Punta del Cobre Formation. West of the Copiapó river, in the Ojancos Nuevo district, the Quebradas Nantoco, Los Algarrobos, and Los Toros, the volcaniclastic Quebrada Los Algarrobos Sequence, in which ammonites of Berriasian age were found (Tilling 1962), appears to directly overlie the Lavas Inferiores. In places the Quebrada Los Algarrobos Sequence is overlain by the Lavas Superiores (Fig. 2).

In the middle Cretaceous, multiple intrusions were emplaced into the Neocomian rocks in the western part of the Punta del Cobre belt (Farrar et al. 1970; Zentilli 1974; Arévalo 1994, 1995), where they caused intense contact metamorphism (Tilling 1962, 1963a, b, 1976; Marschik and Fontboté 1995, 1996). Understanding the timing of intrusion is essential to elucidate the genesis of the ore in the Punta del Cobre belt, not only because of possible genetic relationships but also because of their thermal and metasomatic influence on the area (Marschik and Fontboté 1995, 1996).

Farrar et al. (1970) documented the magmatic history of the Atacama region using the K-Ar technique. Five distinct intrusion episodes in the Permian, Early Jurassic, middle Cretaceous, Early Paleocene and Late Eocene were distinguished. Eastward migration of the magmatic front from Early Jurassic to Late Eocene is indicated by the decreasing age of intrusive bodies from the present coastal region towards the Andean Cordillera. By middle Creta-

►

Fig. 2 Geologic map of the main part of the Punta del Cobre belt (geology modified from Tilling 1976; *a*, lamprophyre; *b*, meladiorite; *c*, diorite; *d*, leucodiorite; *e*, tonalite; *f*, quartz monzonite; *g*, albite granite. The positions of the samples taken for $^{40}Ar/^{39}Ar$, K-Ar, and Rb-Sr analyses are indicated. The stratigraphy of the Punta del Cobre Formation east of the Copiapó river (Punta del Cobre and Ladrillos districts) and west of the river (Ojancos Nuevo district, Quebradas Nantoco, Los Algarrobos, and Los Toros) is summarized in two schematic sections

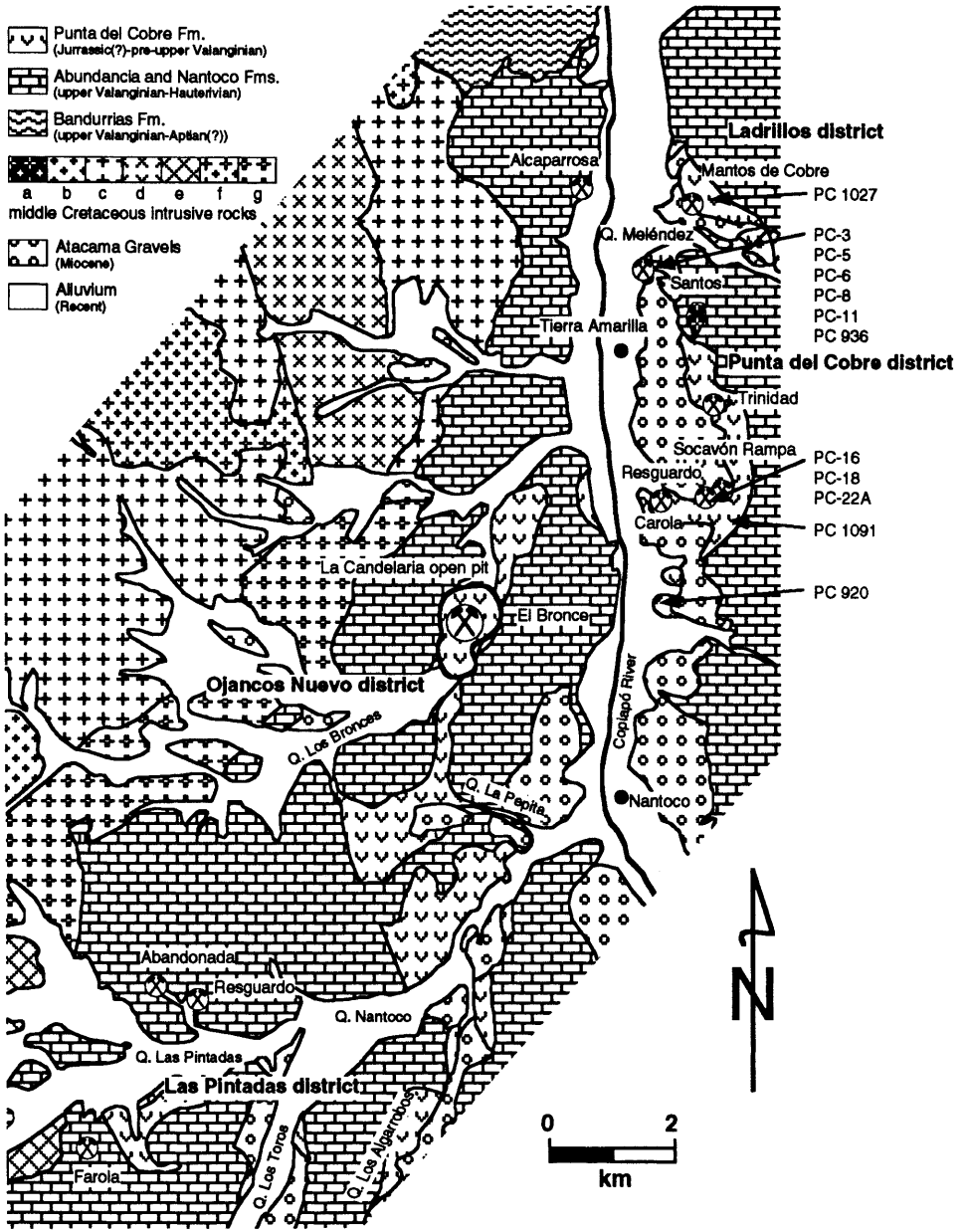
Punta del Cobre Fm.
(Jurrassic(?)-pre-upper Valanginian)
Abundancia and Nantoco Fms.
(upper Valanginian-Hauterivian)
Bandurrias Fm.
(upper Valanginian-Aptian(?))
a b c d e f g
middle Cretaceous intrusive rocks
Atacama Gravels
(Miocene)
Alluvium
(Recent)
Ladrillos district
Alcaparrosa
Mantos de Cobre
PC 1027
Q. Meléndez
PC-3
PC-5
PC-6
PC-8
PC-11
PC 936
Santos
Tierra Amarilla
Punta del Cobre district
Trinidad
Socavón Rampa
PC-16
PC-18
PC-22A
Resguardo
Carola
PC 1091
PC 920
La Candelaria open pit
El Bronce
Ojancos Nuevo district
Q. Los Bronces
Q. La Pepita
Coplapó River
Nantoco
Abandonada
Resguardo
Q. Nantoco
Q. Las Pintadas
Las Pintadas district
Farola
Q. Los Toros
Q. Los Algarrobos
0
2
km

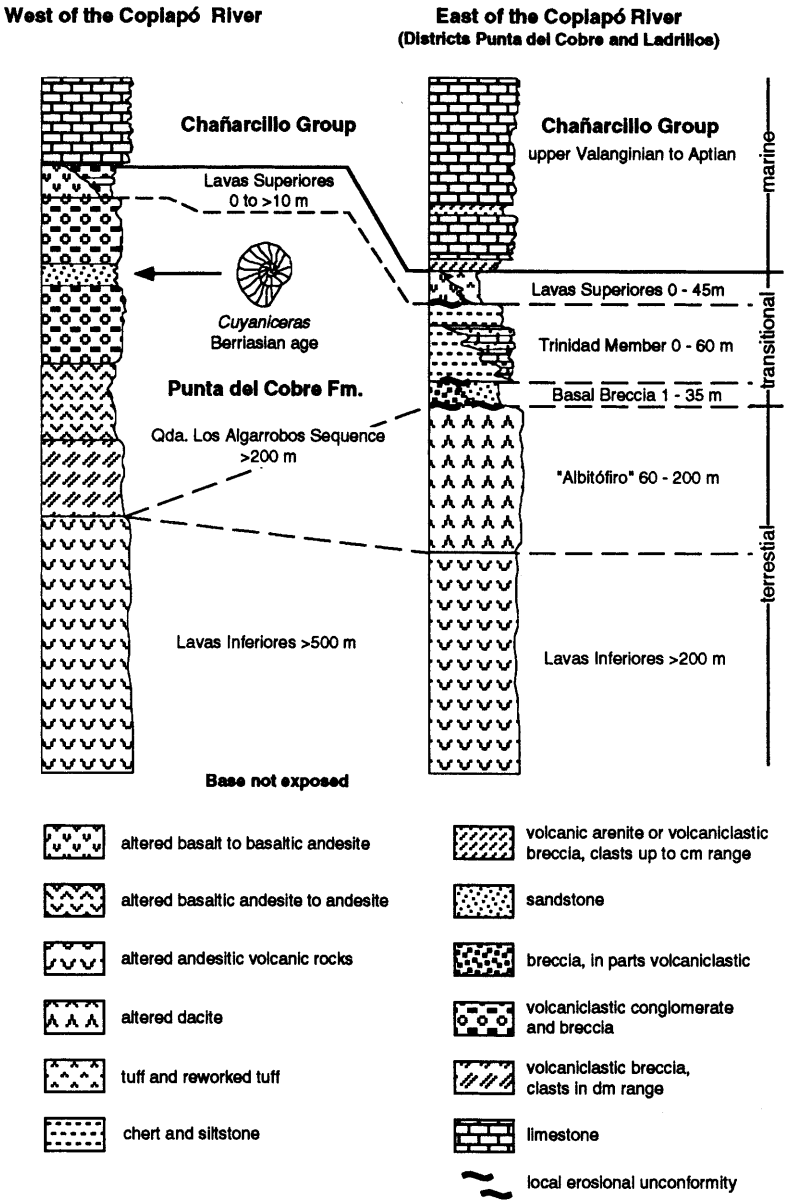
West of the Coplapó River
East of the Coplapó River
(Districts Punta del Cobre and Ladrillos)
Chañarcillo Group
Lavas Superiores
0 to >10 m
Cuyaniceras
Berriasian age
Punta del Cobre Fm.
Qda. Los Algarrobos Sequence
>200 m
Lavas Inferiores >500 m
Chañarcillo Group
upper Valanginian to Aptian
Lavas Superiores 0 - 45m
Trinidad Member 0 - 60 m
Basal Breccia 1 - 35 m
"Albitófiro" 60 - 200 m
Lavas Inferiores >200 m
marine
transitional
terrestial
Base not exposed
altered basalt to basaltic andesite
altered basaltic andesite to andesite
altered andesitic volcanic rocks
altered dacite
tuff and reworked tuff
chert and siltstone
volcanic arenite or volcaniclastic breccia, clasts up to cm range
sandstone
breccia, in parts volcaniclastic
volcaniclastic conglomerate and breccia
volcaniclastic breccia, clasts in dm range
limestone
local erosional unconformity

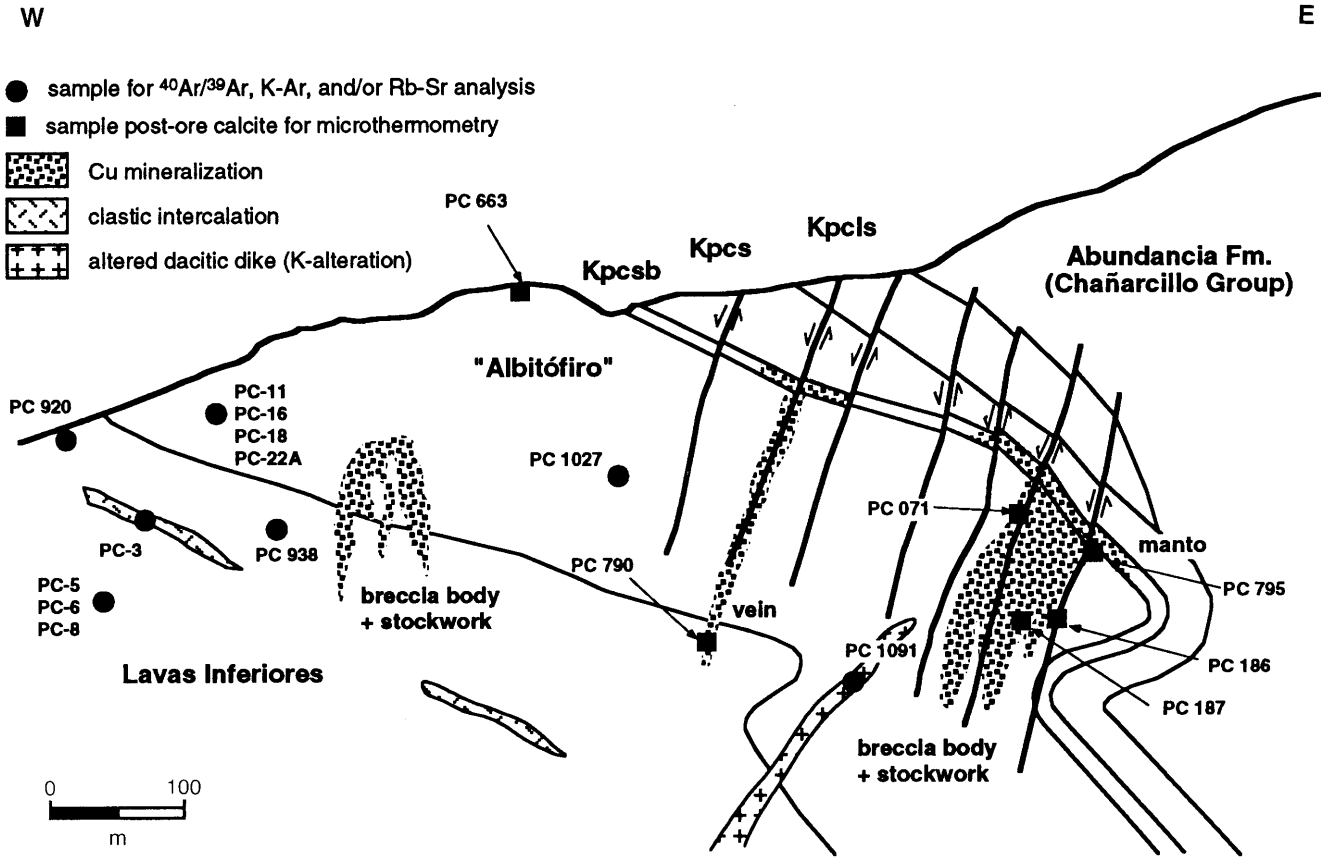

Fig. 3 Geometric ore types in a schematic cross section through the Punta del Cobre district. The relative sample positions are indicated. *Kpcsb*, Basal Breccia; *Kpcs*, Trinidad Member; *Kpcls*, Lavas Superiores

ceous, the intrusion foci were at the longitude of Copiapó (Fig. 1). K-Ar ages for the middle Cretaceous batholith in the Punta del Cobre area range from 119 to 97 Ma (Farrar et al. 1970; Zentilli 1974; Arévalo 1994, 1995); a K-Ar hornblende age of 69 Ma was determined for a granodiorite intruding those batholith rocks (Arévalo 1994). In the Early Paleocene the locus of intrusions was about 25 km east of the Punta del Cobre area (e.g., Cabeza de Vaca plutonic complex). Granodiorites at the Quebradas de los Condores and Cerrillos gave K-Ar biotite ages of 62.4 ± 2.0 Ma and 60.5 ± 1.8 Ma, respectively, whereas diorite at Quebrada Cerrillos yielded a K-Ar hornblende age of 64.7 ± 2.0 Ma (Farrar et al. 1970; Zentilli 1974; all pre-1976 ages converted according to the 1976 IUGS recommendations; Dalrymple 1979).

The magmatic evolution of the middle Cretaceous batholith in the Punta del Cobre area was studied by Tilling (1962, 1963a, 1976). The intrusions range from melanodiorite to albitic sodic granites with predominance of diorite and quartz monzonite (Tilling 1963a, 1976). Field relationships demonstrate that felsic plutons and dikes generally intrude the more mafic rocks. Lamprophyric dikes of unknown age cut all intrusive rocks.

At its eastern margin the batholith is bordered by shear zones and brecciated intrusive rocks that define subvertical contacts, suggesting a structure-controlled forcible emplacement in a quasi-solid state. The emplacement may have occurred in several steps, as indicated by the presence of multiple intrusions of distinct compositions and by the distinguishable superimposed alteration events (Tilling 1962, 1963a, b; Ryan et al. 1994, 1995).

Mineralization and alteration

The mineralization of the Punta del Cobre belt is characterized by a simple primary ore mineral assemblage consisting of chalcopyrite, pyrite, magnetite, and hematite. Gangue is mainly calcite and quartz. In the Punta del Cobre district, Cu ore is mined from breccia bodies, which laterally grade into stockwork and veins, hosted by the volcanic rocks of the Punta del Cobre Formation (Fig. 3; Camus 1980, 1986; Marschik and Fontboté 1996). The concordant stratiform mineralization (manto) is located mainly in the Basal Breccia overlying the volcanic rocks. Average ore grades are about 1.1 to 2 wt.% Cu and may reach more than 8 wt.% Cu in veins. Magnetite occurs together with chalcopyrite and also as massive irregular-shaped bodies and veins (Lino 1984; Hopf 1990; Ryan et al. 1995). East of the Copiapó river (Punta del Cobre and Ladrillos districts), mineralization is controlled by north-northwest- to northwest-trending faults and its upper limit corresponds to the upper contact of the Basal Breccia. In contrast, at the Candelaria deposit, west of the Copiapó river, alteration and mineralization extend into carbonates of the Chañarcillo Group (Ryan et al. 1994, 1995). Ore formation temperatures up to 400 °C to 500 °C were estimated by Hopf (1990) based on the presence of a Ag-Au-Hg amalgam (Nysten 1986) and the observation of intense anisotropy and lance-shaped twin lamellae of chalcopyrite, interpreted to be the result of the inversion

of a high-temperature cubic to a low temperature tetragonal form.

Sulfur isotope compositions of chalcopyrite and pyrite from various deposits of the Punta del Cobre belt range from −0.7 to +2.9‰ in $\delta^{34}S_{CDT}$ values indicating a magmatic sulfur source. The composition of this magmatic sulfur may reflect a component derived via leaching of the underlying volcanic rocks or a direct contribution from magmatic fluids (Marschik et al. 1997). Lead isotope analyses suggest a common source of Pb for the Cu(-Fe)-Au mineralization in the belt and middle Cretaceous batholithic rocks that are exposed in the west of the area (Marschik et al. 1997).

The alteration pattern in the Punta del Cobre belt appears to be controlled by at least two distinct superimposed alteration episodes: (1) hydrothermal alteration and (2) contact metamorphism (Fig. 4; Marschik and Fontboté 1996). Zeolite, prehnite-pumpellyite, and greenschist facies metamorphism occurred in the Mesozoic Andean basin of central Chile (Levi 1970; Aguirre et al. 1978) and may have affected the Punta del Cobre belt. If so, its effects are indistinguishable from chlorite(±epidote) produced by contact metamorphism or hydrothermal alteration.

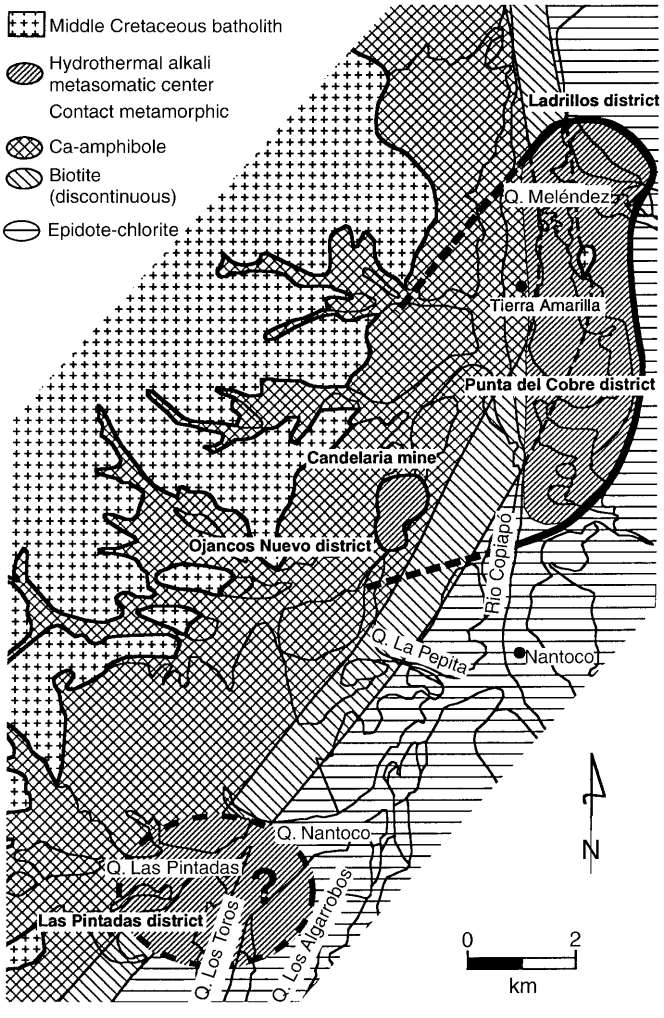

Fig. 4 Schematic representation of the distribution of hydrothermal alteration and contact metamorphism in the volcanic rocks of the Punta del Cobre Formation

Hydrothermal alteration

In the volcanic rocks of the Punta del Cobre Formation, hydrothermal alteration caused extensive albitization followed by potassic alteration. Alkali metasomatism and in particular potassic alteration is spatially associated with Cu(-Fe)-Au mineralization in the entire Punta del Cobre belt. The rocks affected by sodium metasomatism are altered to an assemblage of albite-quartz-chlorite ± sericite ± calcite, whereas rocks affected by potassic alteration mainly contain K-feldspar and/or biotite plus quartz ± chlorite ± sericite ± calcite ± tourmaline. These two different types of pervasive alterations resulted in marked changes in bulk rock chemical composition. Sodic alteration led to Na_2O contents up to 10 wt.% accompanied by a substancial decrease in K_2O (to <0.5 wt.%) and Rb (to <3 ppm). In contrast, potassic alteration, which we infer to occur later in most places led to marked increases in K_2O up to 11 wt.% and Rb up to 250 ppm. With few exceptions, Sr concentrations are low (<100 ppm) and there is no clear evidence for the degree of mobility for Sr evinced by Rb and K_2O.

Contact metamorphism

A later alteration episode reflects contact metamorphism related to the emplacement of the middle Cretaceous batholith in the western part of the area. It produced calc silicate skarn assemblages in the carbonate rocks of the Chañarcillo Group (Tilling 1962, 1963a, b; Ryan et al. 1994, 1995) west of the Copiapó river. In the volcanic rocks of the Punta del Cobre Formation, this alteration occurs as north-northeast-trending and largely overlapping zones characterized by the mineral assemblage Ca-amphibole ± biotite ± sericite proximal to the batholith. Outward from the batholith Ca-amphibole gives way to epidote-chlorite ± quartz ± calcite. These two assemblages overprint areas affected by alkali metasomatism (Marschik and Fontboté 1995, 1996). Petrographic and field evidence suggests that hydrothermal *and* contact metamorphic biotite both occur in the Punta del Cobre area. Whereas hydrothermal biotite, which is closely associated with the ore minerals, was introduced by the hydrothermal alkali-metasomatic event, contact metamorphic biotite occurs in isolated outcrops between the Ca-amphibole and epidote-chlorite zones; these outcrops form a discontinuous biotite zone, characterized by the assemblage biotite ± chlorite ± sericite ± epidote.

Field evidence indicates that the Cu(-Fe)-Au mineralization predates contact metamorphism. The skarn mineral assemblage at the Candelaria mine is post-ore

because it is younger than a post-mineralization phase of shear deformation (Ryan et al. 1994, 1995). A last alteration event partially overlaps retrograde metamorphism and the late stages of mineralization, with K-feldspar apparently overprinting and partially replacing all the previously formed assemblages (Tilling 1963b; Ryan et al. 1994, 1995). This last alteration event is not recognized east of the Copiapó river, i.e., in the Punta del Cobre district sensu strictu.

Gangue minerals

Calcite and chlorite are common gangue minerals in the Punta del Cobre district. In addition to the local carbonatization recognized in the volcanic rocks (e.g., Camus 1980; Hopf 1990; Marschik and Fontboté 1994), calcite, occasionally associated with late specularite, occurs as veins and veinlets cross-cutting mineralized and barren rocks. Calcite veins cut through the upper limit of the mineralization (Basal Breccia) into the Trinidad Member. Calcite veins follow mainly the north-northwest- to northwest-trending structures which control the mineralization, but also northeast, north, and west directions are observed.

Some calcite also fills open spaces between ore minerals. While it is clear that calcite is paragenetically later than the sulfide and iron-oxide mineralization, the time of its precipitation is not known. On the basis of the observations summarized, most calcite postdates the mineralization; thus the fluid from which calcite precipitated was not necessarily related directly to mineralization. This later fluid may have flowed along the same pathway as the mineralizing solution. However, it cannot be excluded that some of the calcite was also precipitated contemporaneously with mineralization.

Chlorite is common in hydrothermally altered and low grade metamorphic rocks. In large parts of the Punta del Cobre district it is a significant constituent, which replaces biotite to various degrees and amphibole or pyroxene completely (Hopf 1990; Marschik et al. 1993). Chlorites are mainly pycnochlorite and ripidolite (Hey 1954) yielding formation temperatures (Cathelineau and Nieva 1985) between 220 °C and 310 °C in orebodies and between 160 °C and 300 °C regionally. The Fe/(Fe + Mg) ratio of the chlorite shows no correlation with the estimated formation temperatures. No systematic changes in chlorite composition towards the mineralized zones or any other particular relationships with the ore minerals are recognized, except that chlorite from orebodies shows higher minimum formation temperatures than those estimated from chlorite found throughout the region (Marschik and Fontboté 1996).

Proposed genetic models

Several different genetic models have been proposed for the ore deposits in the Punta del Cobre belt. Based on investigations mainly in the Punta del Cobre district, Camus (1980) suggested a submarine volcanogenic massive sulfide model in which veins, breccias, and stockwork zones represent feeders for the stratiform mineralization located at their top. Hopf (1990) proposed a mineralization model similar to porphyry copper predating the Basal Breccia. She suggested partial erosion of this mineralization and subsequent clastic deposition of ore minerals in the Basal Breccia. Both models imply that the ore formation occurred before the deposition of the Abundancia Formation, i.e., in pre-upper Valanginian times.

In a generalized overview on Chilean manto type deposits Sato (1984) favored an epigenetic model for several deposits including Punta del Cobre, whereby metamorphic fluids produced by dehydration processes during regional (burial) metamorphism leached copper and sulfur from volcano-sedimentary rocks. Low ore formation temperatures were assumed because of the apparent absence of wall-rock alteration in those deposits and the low trapping temperatures (65 °C to 195 °C) of fluid inclusions in calcite of the Buena Esperanza deposit (Nisterenko et al. 1973). Later investigations showed that the ore deposits of the Buena Esperanza–Carolina de Michilla belt formed at much higher temperatures (350 °C–500 °C) and with intense hydrothermal alteration (Palacios 1990; Wolf et al. 1990).

The similarity between Punta del Cobre and porphyry copper deposits had apparently already been proposed by Flores in 1942 (Segerstrom and Ruiz 1962). Segerstrom and Ruiz (1962) stated that the deposits could be described as a transition between a porphyry copper and a vein type deposit. Ryan et al. (1994, 1995) emphasized the complex metamorphic and metasomatic history of the Candelaria deposit and noted that this "apparently caused redistribution of the mineralization and probably destroyed much of the information related to its origin. The large size, simple mineralogy and association of early mineralization with potassic alteration suggests that the deposit may have originally been a deep-seated porphyry copper deposit but no direct evidence for this has been found."

Marschik and Fontboté (1995, 1996) concluded that alteration pattern, geometry of the orebodies, ore formation temperatures of about 400 °C to 500 °C, and the sulfur isotope signature all indicate a mineralization event in association with deep-seated magmatic intrusion(s), that was post-Basal Breccia and predates the main stage of batholith emplacement. This conclusion is supported by the presence of mineralization and alteration affecting the base of the Chañarcillo Group west of the Copiapó river, and by the shearing of the Candelaria ore, predating contact metamorphism (Ryan et al. 1994, 1995). Although the Punta del Cobre district could represent an external part of a system similar to those of porphyry copper deposits, the large amounts of magnetite found in the ore of the Punta del Cobre belt suggest a comparison with the magnetite(-apatite)

deposits of the "Chilean iron belt", hosted by Neocomian rocks in the vicinity of middle Cretaceous intrusions (Bookstrom 1977; Pincheira 1985, 1991; Espinoza 1990; Ménard 1992, 1995). These magnetite(-apatite) deposits are frequently characterized by the presence of skarn parageneses. Age of the mineralization (Lower to middle Cretaceous) and ore formation temperatures (475 °C–600 °C) are similar to those recognized in the Punta del Cobre district. Thus we consider that the Cu(-Fe)-Au deposits of the Punta del Cobre belt are members of a family of intrusion-related deposits comprising porphyry copper, magnetite(-apatite), and Fe and Cu-Fe skarn deposits (Marschik and Fontboté 1996). Specifically, the Punta del Cobre district is genetically interpreted to occupy a transitional position between the ores of the Andean magnetite(-apatite) belt and porphyry copper deposits. It is considered probable that the mineralization is related to an unexposed hornblende-bearing batholithic diorite intrusion, which according to Tilling (1962) underlies the Candelaria area (Marschik and Fontboté, 1996).

Each model discussed implies specific temporal relations between host-rock deposition and mineralization. In particular, the models of Camus (1980) and Hopf (1990) predict mineralization predating deposition of the Abundancia Formation. Age determinations presented later allow us to test the validity of these models.

Sampling and analytical techniques

$^{40}Ar/^{39}Ar$, K-Ar and Rb-Sr analyses were performed on rock samples of the Punta del Cobre Formation collected in the Santos (PC-3, PC-5, PC-6, PC-8, PC-11, PC 938), Resguardo (PC-16, PC-18, PC-22A), and Mantos de Cobre (PC 1027) mines. A surface sample of the Lavas Inferiores from an outcrop about 2 km south of the mine installations of Carola mine (PC 920) and another from a K-metasomatized dacitic dike (PC 1091) in the Carola mine are also included in the sample set. Separating pure K-feldspar or biotite from most samples is impossible because of the fine grain size and the complex intergrowth among alteration minerals, therefore, whole-rock samples were chosen for $^{40}Ar/^{39}Ar$ and K-Ar analysis. Whole-rock samples PC-5 and PC-22A contain about 40 to 50% and 15 to 20% biotite, respectively, whereas samples PC 1027 and PC 1091 are dominated by K-feldspar, contain minor amounts of sericite, chlorite, and lack biotite. Sample PC 920 contains K-feldspar, sericite, and biotite that is replaced by chlorite that comprises 5 to 10% of the whole-rock. Samples of post-ore calcite were taken in the Carola and Socavón Rampa mines and from a surface outcrop near the Trinidad mine (Fig. 2). The relative positions of all samples are shown in a schematic cross-section through the Punta del Cobre district (Fig. 3).

Incremental-heating experiments were carried out on three whole-rock (PC 920, PC 1027, PC 1091) and one biotite sample (PC 938) at the University of Geneva $^{40}Ar/^{39}Ar$ Geochronology Laboratory. Whole-rock samples between 0.18 and 0.44 mg and a biotite separate of 0.45 mg were placed into aluminum foil packets and sealed in an evacuated quartz vial along with neutron flux monitor packets. The monitor mineral was biotite HDB-1, which has a recommended K-Ar age of 24.21 ± 0.32 Ma (Lippolt and Hess 1994). A multi-grain $^{40}Ar/^{39}Ar$ incremental-heating analysis of this standard gave a plateau age of 24.292 ± 0.032 Ma, relative to 27.92 Ma Taylor Creek Rhyolite sanidine (Wijbrans et al. 1995). Because the monitor packages were analyzed by incremental-heating, with the mean $^{40}Ar/^{39}Ar$ ratio from five to six plateau steps used to calculate each point of the J-curve, we have calculated our ages relative to 24.292 Ma. The samples were irradiated for 18 h at the Oregon State University Triga reactor in the unlined inner core facility where they received a total fast neutron dose of $\sim 1.6*10^{18}$ n/cm^2. Reactor corrections are as follows: $[^{40}Ar/^{39}Ar]_K = 0.00465$; $[^{36}Ar/^{37}Ar]_{Ca} = 0.000268$; $[^{39}Ar/^{37}Ar]_{Ca} = 0.000698$. The procedures for gas extraction, mass spectrometry, calculation of J values, and criteria for the interpretation of the experimental results are given in Singer and Pringle (1996).

Laser total-fusion $^{40}Ar/^{39}Ar$ analyses of biotite were performed at the Berkeley Geochronology Center using techniques of Deino and Potts (1990). For each analysis, six or seven biotite grains were collectively fused. Calculated ages represent total gas ages and are therefore equivalent to conventional K-Ar age determinations. Whole-rock Rb-Sr and K-Ar analyses were carried out at the Centro de Pesquisas Geocronológicas, University of São Paulo. Whole-rock Rb and Sr contents were determined by X-ray fluorescence or, for samples with low Rb and Sr contents, by a mass-spectrometric isotope dilution technique using ^{84}Sr and ^{87}Rb tracers. Strontium isotope measurements were made in a TH-5 Varian MAT solid source mass spectrometer. The $^{87}Sr/^{86}Sr$ ratios were normalized to a $^{86}Sr/^{84}Sr$ ratio of 0.1194. The Eimer and Amend Sr standard yielded a $^{87}Sr/^{86}Sr$ ratio of 0.7082 ± 0.0013 ($\pm 1\sigma$). Isochron regression was calculated according to York (1966). For the K-Ar age determinations, Ar was measured using standard isotope dilution techniques. Argon isotope analysis was done in a Nuclide MS-1 mass spectrometer. Potassium was measured by flame photometry using a lithium internal standard. All ages were calculated with the decay constants of Steiger and Jäger (1977); errors are reported at the $\pm 2\sigma$ level.

Microthermometric measurements were made on 30 to 50 μm thick double polished wafers with a Fluid Inc. adapted U.S.G.S. gas-flow heating/freezing stage (Woods et al. 1981; Roedder 1984) mounted on a Leitz Laborlux S microscope equipped with a Nikon ELWD long focus lens. The system was calibrated with synthetic fluid inclusions (Sterner and Bodnar 1984) at temperatures of −56.6 °C, 0.0 °C and 374.1 °C. Precision and accuracy are ±0.1 °C between −70 °C and 40 °C, ±2 °C below −70 °C, and ±1 °C above 100 °C.

Chronology

$^{40}Ar/^{39}Ar$ incremental-heating experiments

$^{40}Ar/^{39}Ar$ incremental-heating results are summarized in Table 1 and complete data for two samples are given in the Appendix. The incremental-heating experiment performed on biotite separated from sample PC 938 gave a 12-step plateau that contains 96.4% of the total released ^{39}Ar, yielding an age of 114.6 ± 0.8 Ma. These plateau steps define an inverse isochron age of 114.9 ± 1.0 Ma with an $^{40}Ar/^{36}Ar$ intercept of 291.2 ± 5.3. Whole-rock samples PC 920, PC 1027, and PC 1091 yielded plateau ages of 90.2 ± 0.6 Ma, 89.5 ± 0.6 Ma, and 89.8 ± 0.6 Ma, including 11, 7, and 6 plateau steps (Fig. 5; Table 1). The 11 plateau steps of sample PC 920 define an inverse isochron age of 90.7 ± 1.2 Ma with an $^{40}Ar/^{36}Ar$ intercept of 287.8 ± 6.9. For samples PC 1027 and PC 1091, an insufficient spread in $^{40}Ar/^{39}Ar$ ratio precluded isochron analysis. The isochron ages are preferred over the plateau ages because they combine quantitative estimates of analytical precision plus the internal disturbance of the sample and they make no assumption about the trapped argon component (e.g., Singer and Pringle 1996).

Table 1 Summary results of $^{40}Ar/^{39}Ar$ incremental-heating analyses

Sample	Location	Unit	Material	Total-fusion age (Ma) ± 2σ	Age spectrum			Inverse isochron			
					Increments used (°C)	^{39}Ar (%)	Age ± 2σ (Ma)	N	$\frac{SUMS}{(N-2)}$	$^{40}Ar/^{36}Ar$ intercept[b]	Age ± 2σ (Ma)
PC 938	Santos, N310	Lavas Inferiores	Biotite	114.1 ± 1.0	850–1300	96.4	114.6 ± 0.8	12 of 14	0.25	291.2 ± 5.3	114.9 ± 1.0
PC 920	Carola, Cobriza	Lavas Inferiores	Whole-rock	91.8 ± 1.0	900–1260	55.8	90.2 ± 0.6	11 of 21	1.94	287.8 ± 6.9	90.7 ± 1.2
PC 1027	Mantos de Cobre	"Albitófiro"	Whole-rock	90.1 ± 0.6	800–1000	53.3	89.5 ± 0.6	7 of 13	insufficient spread in data		
PC 1091	Carola, N11	Dike	Whole-rock	87.6 ± 0.6	905–1250	62.0[a]	89.8 ± 0.6	7[a] of 13	insufficient spread in data		

All ages calculated relative to HDB-1 biotite (24.292 Ma; Wijbrans et al. 1995), using decay constants of Steiger and Jäger (1977)

[a] One plateau step lost, roughly 8% of gas

[b] $^{40}Ar/^{36}Ar$ intercept errors are ± 1σ

All release spectra show a progressive increase in age in the low temperature steps over the first 5 to 15% of gas released (Fig. 5). The shape of the spectra is a complex function of mineralogy, grain size, and subsequent cooling rate. The low apparent ages associated with the lowest temperature gas release may reflect a variety of factors including Ar loss and/or ^{39}Ar recoil from fine-grained phases. Not surprisingly, the mineralogically most complex whole-rock sample PC 920 gave the most discordant age spectrum. The older ages comprising about 30% of the gas released at low temperature give apparent ages roughly 7% higher than the calculated plateau age. These high apparent ages and the staircase downward progression into the plateau segment of the release spectra may reflect ^{39}Ar recoil from fine-grained chlorite and sericite (e.g, McDougall and Harrison 1988, pp 110–113).

K-Ar, Rb-Sr and $^{40}Ar/^{39}Ar$ total-fusion analyses

Three $^{40}Ar/^{39}Ar$ laser total-fusion analyses of biotite from the Resguardo mine yielded ages of 114.6 ± 1.6 Ma for sample PC-16 and a weighted mean age of 111.6 ± 1.4 Ma for PC-22A (Table 2). Whole rock K-Ar analyses gave ages of 101.5 ± 1.8 Ma (PC-22A, Resguardo mine) and 109.7 ± 1.6 Ma (PC-5, Santos mine). A whole-rock Rb-Sr isochron calculated from seven samples give 116.8 ± 2.7 Ma (Fig. 6; Table 3).

Microthermometry of fluid inclusions

Fluid inclusion types and behavior during microthermometric measurements

Three fluid inclusion types in late calcite were observed at room temperature: two phase inclusions (type I) containing a liquid and a vapor phase, three phase inclusions (type II) with liquid, vapor, and one visible solid phase, and light or dark colored single phase inclusions (type III). Most of the fluid inclusions are ≤30 μm in size and typically inclusions between 8 and 20 μm were examined. Type I and type II inclusions show fairly uniform vapor-liquid ratios. Irregular, negative euhedral, drop, and tube shaped inclusions were observed.

During the microthermometric measurements freezing could often not be achieved and even supercooling to −190 °C did not result in freezing of the fluid inclusion. However, during warming from temperatures below −120 °C freezing of type II inclusions sometimes occurred between −80 °C to −60 °C.

Many type I inclusions are actually metastable type II inclusions that failed to nucleate a daughter crystal. Both types show similar liquid homogenization (Th_{liquid}) and final ice melting temperatures (Tm_{ice}). In the rare

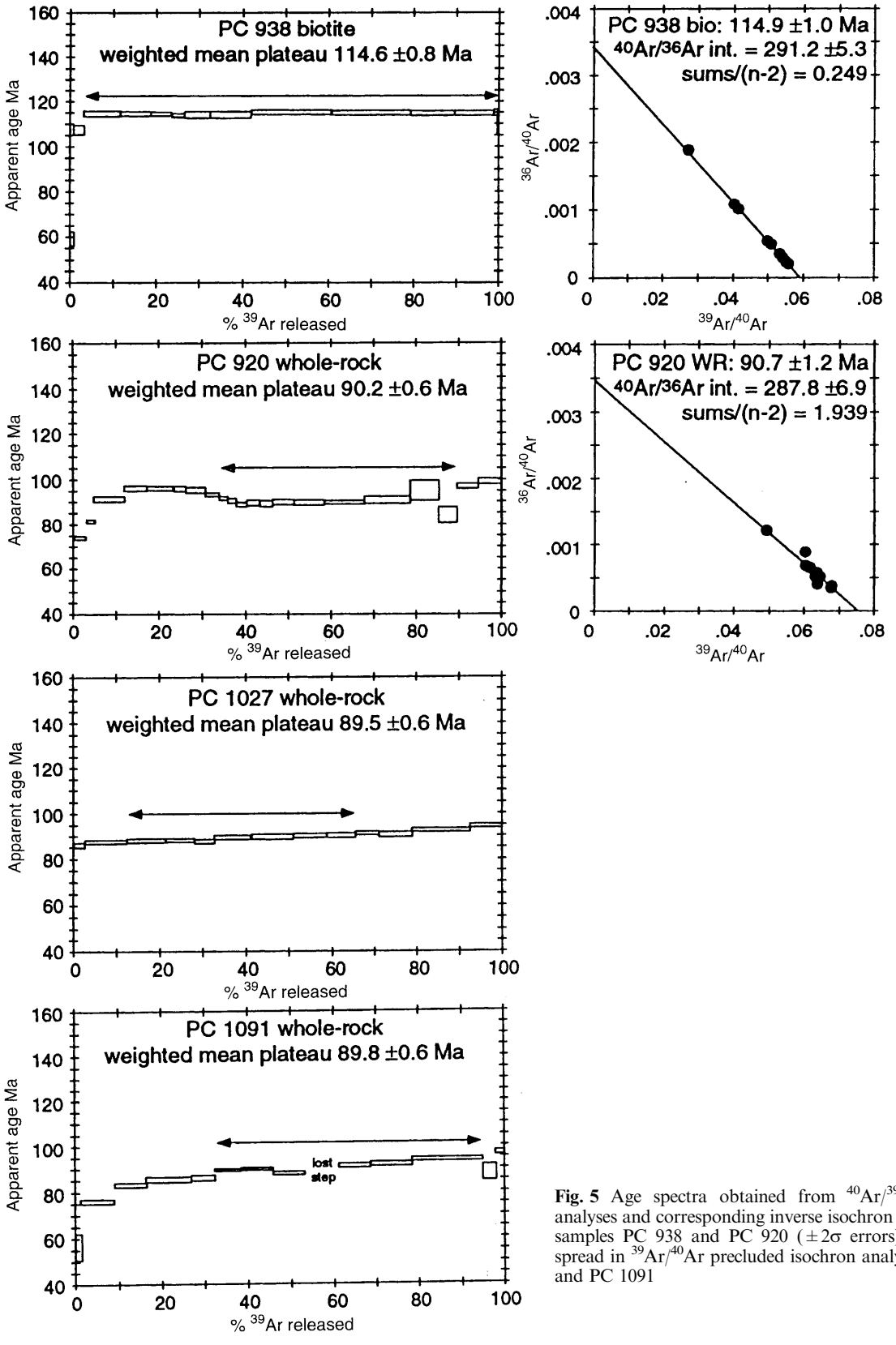

Fig. 5 Age spectra obtained from $^{40}Ar/^{39}Ar$ incremental-heating analyses and corresponding inverse isochron correlation diagrams for samples PC 938 and PC 920 ($\pm 2\sigma$ errors). Note that insufficient spread in $^{39}Ar/^{40}Ar$ precluded isochron analyses of samples PC 1027 and PC 1091

Table 2 Results of $^{40}Ar/^{39}Ar$ biotite total-fusion and K-Ar whole-rock analyses

Sample	Location	Unit	Material	Method[a]	Apparent age ± 2σ (Ma)
PC-16	Resguardo	"Albitófiro"	Biotite	$^{40}Ar/^{39}Ar$ total-fusion	114.6 ± 1.6
PC-22A	Resguardo	"Albitófiro"	Biotite	$^{40}Ar/^{39}Ar$ total-fusion	111.2 ± 1.8
PC-22A	Resguardo	"Albitófiro"	Biotite	$^{40}Ar/^{39}Ar$ total-fusion	112.4 ± 2.4
				Mean age[b]	111.6 ± 1.4
PC-5	Santos	Lavas Inferiores	Whole-rock	K-Ar	109.7 ± 1.6
PC-22A	Resguardo	"Albitófiro"	Whole-rock	K-Ar	101.5 ± 1.8

[a] $^{40}Ar/^{39}Ar$ ages calculated relative to Fish Canyon Tuff sanidine (28.84 Ma; Cebula et al. 1986)
[b] Weighted by inverse of the variance (see Singer and Pringle 1996)

Table 3 Rb-Sr analyses of whole-rock samples from the Punta del Cobre district

Sample	Location	Unit	Rb ppm	Sr ppm	$^{87}Rb/^{86}Sr$	$^{87}Sr/^{86}Sr$
PC-3	Santos	Lavas Inferiores?	182	77	6.800 ± 0.192	0.71601 ± 0.00003
PC-5	Santos	Lavas Inferiores	46	89	1.501 ± 0.042	0.70740 ± 0.00004
PC-6	Santos	Lavas Inferiores	89	77	3.360 ± 0.095	0.71029 ± 0.00029
PC-8	Santos	Lavas Inferiores?	163	69	6.892 ± 0.195	0.71596 ± 0.00003
PC-11	Santos	"Albitófiro"	114	211	1.564 ± 0.044	0.70727 ± 0.00003
PC-18	Resguardo	"Albitófiro"	68	46	4.388 ± 0.124	0.71214 ± 0.00008
PC-22A	Resguardo	"Albitófiro"	68	68	2.696 ± 0.075	0.70952 ± 0.00003

Rb-Sr isochron age = 116.8 ± 2.7 Ma (±2σ); initial ratio = 0.70482 ± 0.00009; MSWD = 1.8

cases when freezing of type I inclusions could be achieved a solid phase formed in some inclusions after they reached room temperature. On the other hand, after dissolving the solid phase, many type II inclusions persist in this metastable two-phase state (liquid + vapor) and could not be frozen during the following cooling runs.

Type II inclusions usually homogenized at temperatures lower than the dissolution of the solid phase (Td_{solid}). Decrepitation often occurred at relatively low temperatures, i.e., below Td_{solid} and the inclusions changed their appearance and looked similar to the dark, type III inclusions. Since no phase changes were observed in the latter during the measurements they might represent inclusions that had already decrepitated.

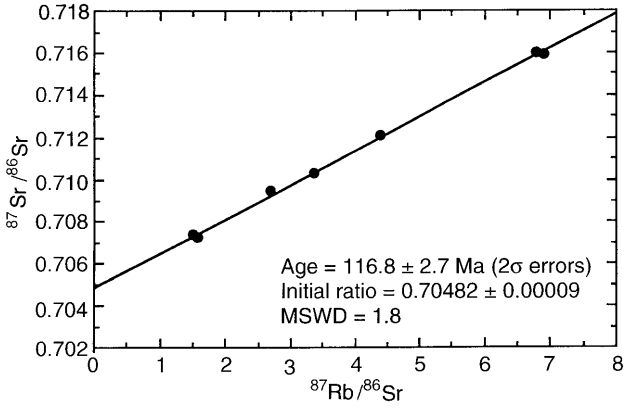

Fig. 6 Rb-Sr isochron calculated from seven whole-rock samples (note that figures are given at ±2σ errors)

Results

Liquid homogenization temperatures of type I inclusions range between 78 °C and 167 °C and final ice melting temperatures between −29 °C and −40 °C. Type II inclusions show Th_{liquid} from 100 °C to 175 °C and complete homogenization (Td_{solid}) between 136 °C and 232 °C. Final ice melting temperatures fall between −28 °C and −47 °C. A graphic summary of the data is given in Fig. 7a–c. The cube-shape of the daughter crystal in type II inclusions suggests that it is halite. Total salinities ($NaCl_{equiv.}$) of type II inclusions were calculated using the equation of Potter et al. (1977). They vary between 29.2 and 33.6 wt.% $NaCl_{equiv.}$ (Fig. 7d). Initial ice melting typically occurred below −55 °C suggesting the presence of cations other than Na^+, such as Ca^{2+}. The trapped fluids therefore belong to the system H_2O-NaCl-$CaCl_2$. The formation of antarcticite was not observed and hydrohalite only occasionally was recognized.

The fluid composition of type II inclusions of selected samples was graphically estimated (Williams-Jones and Samson 1990) and found to contain 12 to 24 wt.% NaCl and 13 to 23 wt.% $CaCl_2$. Isochores were calculated based on averaged values with the MacFlinCor program (Brown and Hagemann 1995) considering a mixed salt system containing NaCl and $CaCl_2$ in H_2O (Fig. 8). Assuming a middle Cretaceous age for the formation of the post-ore calcite veins, burial was most likely 2–3 km. Thus, the isochores indicate formation temperatures for post-ore calcite between 125 °C and 175 °C assuming hydrostatic, or between 150 °C and 205 °C for lithostatic pressure conditions. The spread of the data in

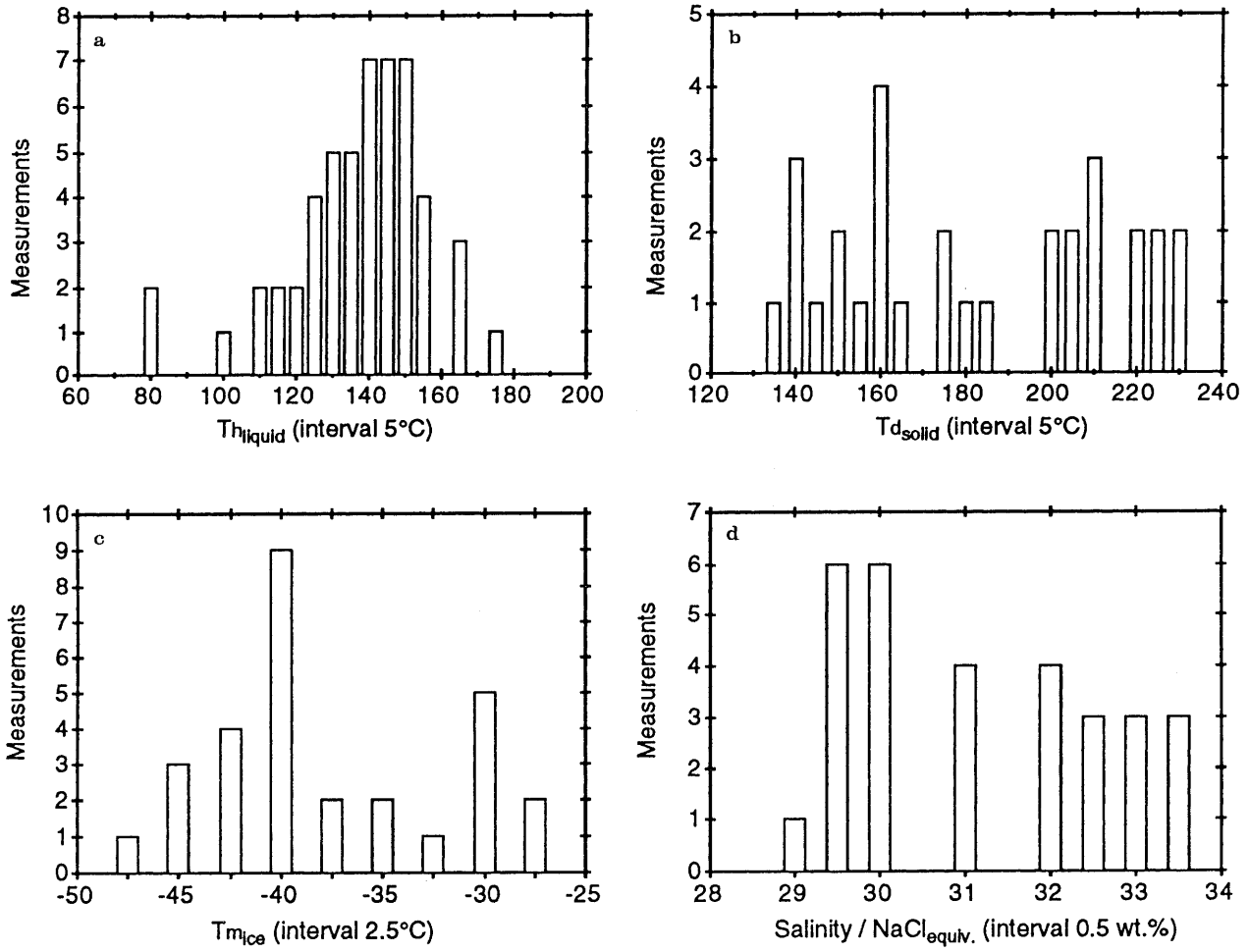

Fig. 7a–d Results of microthermometric measurements: **a** liquid homogenization temperatures at which a solid phase is usually still present in type II inclusions; **b** solid dissolution temperature, i.e., complete homogenization to a liquid phase; **c** final ice melting temperature; **d** calculated salinities ($NaCl_{equiv.}$) using the equation of Potter et al. (1977). See Fig. 3 for relative sample positions

Fig. 7 may be in part be the result of stretching of the host mineral (Roedder 1984).

The homogenization temperatures obtained are similar to those presented by Rabbia et al. (1996) for calcite from the Carola mine (Th_{liquid} between 175 °C and 236 °C). Carbon and oxygen isotopic composition of the same samples between −8.7 and −9.4‰ $\delta^{13}C$ (PDB) and between 15.4 and 15.9‰ $\delta^{18}O$ (SMOW; Rabbia et al. 1996). Calculated isotopic compositions of a fluid in equilibrium with calcite indicate $\delta^{18}O$ values between 4.6 and 7.7‰ for a temperature range of 175 °C to 235 °C (using isotope fractionation factors of Friedman and O'Neil 1977). These values are consistent with magmatic fluids or with fluids equilibrated with magmatic silicates at high temperature.

Discussion

The exact age of the lower volcanic unit (Lavas Inferiores and "Albitófiro") of the Punta del Cobre Formation is uncertain because of the absence of time markers and the erosional unconformity at its top (Marschik and Fontboté 1996). On the basis of lithostratigraphic correlations a Jurassic(?) to Berriasian age is probable. Ammonites of Berriasian age are found in the Quebrada Los Algarrobos Sequence (Tilling 1962) and a Berriasian to pre-upper Valanginian age is assumed for the Lavas Superiores, since they in places overlie the Quebrada Los Algarrobos Sequence and in turn are overlain by the Abundancia Formation (upper Valanginian near its top, based on paleontological findings; Corvalán 1974). Therefore, the volcanic rocks of the Punta del Cobre Formation are of pre-upper Valanginian age, i.e., older than ~125–130 Ma (Cowie and Bassett 1989).

Alkali metasomatism and in particular potassic alteration is spatially associated with mineralization in the Punta del Cobre belt. Therefore, dating the formation of biotite, K-feldspar, and sericite provides constraints on the age of alteration related to ore formation. Isotopic ages of the analyzed altered whole-rocks and mineral separates span a range from 89.5 to 116.8 Ma. The $^{40}Ar/^{39}Ar$ inverse isochron age of hydrothermal biotite associated with mineralization (114.9 ± 1.0 Ma, PC 938; Fig. 5) is the most reliable evidence concerning the

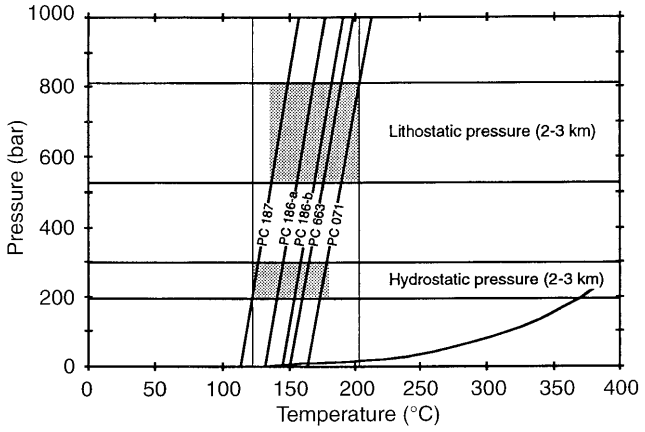

Fig. 8 Calculated isochores assuming lithostatic (~0.5–0.8 kbar; 2 to 3 km burial) and hydrostatic pressure (~0.2–0.3 kbar; 2 to 3 km burial). The isochores provide a probable calcite formation temperature range between 122.5 °C and 174.1 °C at 0.2 kbar and 148.8 °C and 203.3 °C at 0.8 kbar pressures. Sample *PC 186* shows two distinguishable populations of inclusions which are indicated as *PC 186-a* and *PC 186-b*

date of the mineralization. The age of this hydrothermal biotite shows that ore deposition is coeval with the earlier stages of batholith formation in the Punta del Cobre area (range of K-Ar ages from 119 to 97 Ma for the middle Cretaceous batholith, Farrar et al. 1970; Zentilli 1974; Arévalo 1994, 1995). This is consistent with the field observation that the post-ore and post-shear skarn mineral assemblage at Candelaria was produced by contact metamorphism during the later, main stage of batholith emplacement (Ryan et al. 1994, 1995).

The whole-rock Rb-Sr isochron age of 116.8 ± 2.7 Ma (Table 3) is indistinguishable within error from the biotite $^{40}Ar/^{39}Ar$ inverse isochron age and one biotite laser total-fusion $^{40}Ar/^{39}Ar$ age (114.9 ± 1.0 and 114.6 ± 1.6 Ma, respectively). It is not clear what accounts for the 111.6 ± 1.4 Ma age of biotite from sample PC-22A. The small difference in age may reflect variable purity of the mineral separates or possibly the duration of hydrothermal activity in this area. Verification of the latter will require further investigation. The Rb-Sr isochron age most probably reflects the resetting of the Rb-Sr isotope system concurrent with the timing of mineralization, the latter recorded by the hydrothermal biotite of sample PC 938. This is due to the introduction of Rb and K_2O during potassic alteration that followed severe depletion of these elements during earlier sodic alteration.

The polymineralic nature of the whole-rock samples makes the interpretation of the $^{40}Ar/^{39}Ar$ and K-Ar analysis challenging. Whole-rock K-Ar ages of 109.7 ± 1.6 Ma (PC-5) and 101.5 ± 1.8 Ma (PC-22A; Table 2) are considerably older than the three $^{40}Ar/^{39}Ar$ ages from K-feldspar-rich whole-rocks (PC 920, PC 1027, PC 1091; Table 1), possibly reflecting the relative proportion of biotite and K-feldspar. Biotite has a higher closure temperature for retention of argon (~300 °C to 350 °C) than K-feldspar (~150 °C; McDougall and Harrison 1988). Therefore, biotite-rich whole-rocks were more resistant to thermal resetting and record older ages than do the K-feldspar-rich whole-rock samples. The latter samples are interpreted to reflect cooling below 200 °C–150 °C at about 90 Ma.

The $^{40}Ar/^{39}Ar$ age determinations give insight to the thermal history of the area. Figure 9 is a graphical compilation based on our best age data. These data indicate that potassic alteration, which is superimposed on intense albitization, took place at the end of the Neocomian (after the IUGS time scale of Cowie and Bassett 1989) or Aptian (time scale of Harland et al. 1990) coeval with the early stages of batholith formation. Ore minerals were deposited at temperatures of 400 °C to 500 °C. Shearing at the Candelaria deposit occurred after mineralization and before the main stage of batholith emplacement. The biotite ages (PC 938, PC-16, PC-22A; Tables 1 and 2) indicate that the Punta del Cobre district, in contrast to the area west of the Copiapó river, was unaffected by thermal contact metamorphism above ~300 °C to 350 °C, the closure temperature of biotite (McDougall and Harrison 1988). This is consistent with estimated formation temperatures of chlorite (160 °C–310 °C) and the temperatures obtained from fluid inclusions of post-ore calcite. The uniform $^{40}Ar/^{39}Ar$ ages obtained from samples PC 920, PC 1027, and PC 1091 point to subsequent regional cooling below 200 °C–150 °C, the argon closure temperatures of the K-feldspar dominated whole-rock samples, at around 90 Ma, concomitant with regional uplift. K-Ar ages for batholithic intrusions suggest a period of Early Paleocene magmatism (Farrar et al. 1970; Arévalo 1994). Although the relatively low apparent ages form low temperature portions of the Ar release spectra of samples PC 938, PC 920 and PC 1091 (Fig. 5) may be consistent with later reheating, the Ar ages may reflect other complexities discussed earlier. Further work will be neccessary to determine the effects, if any, of Paleocene reheating on Ar systematics.

The relatively high salinity (12–24 wt.% NaCl and 13–23 wt.% $CaCl_2$) and calculated isotopic compositions of fluid inclusions found in post-ore calcite suggest the participation of magmatic fluids. Late stage fluids related to the mineralizing hydrothermal system or, alternatively, to the intrusion of the batholith may explain these salinities and isotopic fluid compositions.

The results of this study are incompatible with genetic models based on the assumption that the ore was formed before the deposition of the Abundancia Formation, i.e., in pre-upper Valanginian times, summarized already, and do not support the metamorphic model of Sato (1984). The data are consistent with an epigenetic model of a hydrothermal system associated with magmatic intrusion(s) that is related to the earlier stages of middle Cretaceous batholith emplacement in the Copiapó area. Therefore, the mineralization is probably related to mafic, in particular, hornblende-bearing dioritic magmas, which predominated during these early stages of

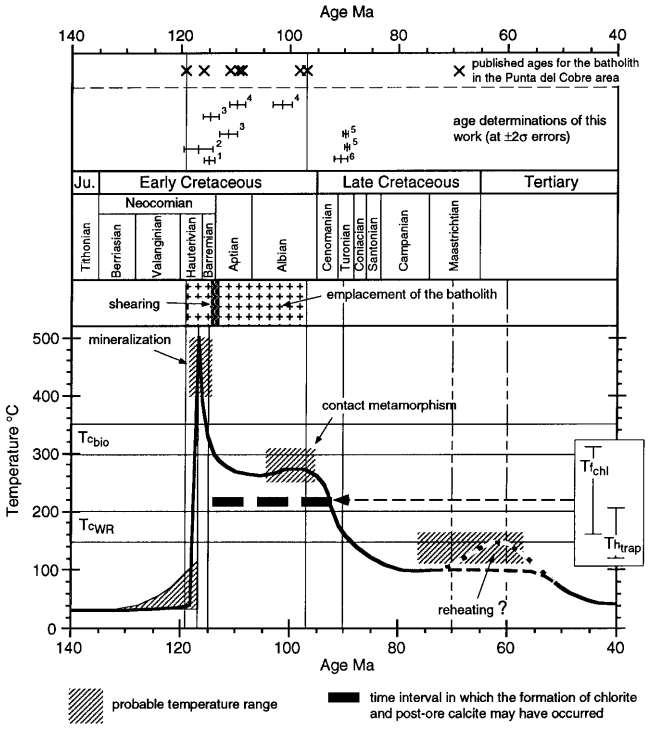

Fig. 9 Schematic representation of the Cretaceous to Paleocene thermal and metasomatic history of the Punta del Cobre district. Age data: *1*, biotite $^{40}Ar/^{39}Ar$ inverse isochron age of 114.9 ± 1.0 Ma; *2*, Rb-Sr-isochron age 116.8 ± 2.7 Ma; *3*, biotite $^{40}Ar/^{39}Ar$ total-fusion age of 114.6 ± 1.6 Ma, and weighted mean age (2 samples) of 111.6 ± 1.4 Ma; *4*, whole-rock K-Ar ages of 109.7 ± 1.6 and 101.5 ± 1.8 Ma; *5*, whole-rock $^{40}Ar/^{39}Ar$ plateau ages of 89.8 ± 0.6 and 89.5 ± 0.6 Ma; *6*, whole-rock $^{40}Ar/^{39}Ar$ inverse isochron age of 90.7 ± 1.2 Ma; *crosses*: age data for the batholith in the Copiapó area from Farrar et al. (1970) and Arévalo (1994, 1995). Abbreviations: Tc_{bio}: closure temperature for biotite according to McDougall and Harrison (1988); Tc_{WR}: probable closure temperature for the whole-rock samples; Tf_{chl}: range of estimated chlorite formation temperatures; Th_{trap}: range of minimum trapping temperatures of fluid inclusions in post-ore calcite assuming pressure between 0.2 and 0.8 kbar. Stratigraphic ages according to the IUGS compilation of Cowie and Bassett (1989). Note that if the time scale of Harland et al. (1990) is used the mineralization would have taken place in Aptian times

batholith formation and which were followed by more felsic plutons (Tilling 1962).

Although the deposits of the Punta del Cobre belt share features with external parts of porphyry copper systems, a middle Cretaceous age is rather unusual for porphyry copper deposits in the central Andes. The only example is at Andacollo (Munizaga et al. 1985; Sillitoe 1988). Concerning age, setting, host rocks, ore geometry, and, alkaline and calcsilicate alteration, deposits of the "Chilean iron belt" are remarkably similar to those of the Punta del Cobre belt and the latter may only represent a variation of these hydrothermal systems.

Deposits like those in the Punta del Cobre belt are probably more widespread in the Andean region and it may be due to chance geologic circumstances that other examples have yet to be found. As more thermochronologic data is available we may recognize regional differences and better place these deposits in a broader geologic context.

Conclusions

Our age determinations using different analytical techniques are consistent considering the analytical precision and the parameters controlling the retention of argon in the whole-rock samples. The $^{40}Ar/^{39}Ar$ biotite age determinations (114.9 ± 1.0 Ma and 114.6 ± 1.6 Ma) and the Rb-Sr isochron (116.8 ± 2.7 Ma) date potassic alteration, which accompanies the mineralization and therefore gives the age of ore deposition. The K-Ar and Rb-Sr systems in these rocks were not modified by heating due to contact metamorphism during subsequent emplacement of post-ore batholithic intrusions. $^{40}Ar/^{39}Ar$ whole-rock ages (90.7 ± 1.2 Ma, 89.8 ± 0.6 Ma, and 89.5 ± 0.6 Ma) represent cooling concomitant with uplift of the area. These new data imply that mineralization is coeval with the initial stages of batholith emplacement and strongly suggest that ore formation is genetically related to it. The data support the hypothesis that the Punta del Cobre belt belongs to the family of intrusion-related deposits comprising porphyry copper, magnetite(-apatite), and Fe and Cu-Fe skarn deposits.

Acknowledgements We thank Cía. Minera Copiapó/COMINOR, Cía. Minera Ojos del Salado S.A., Sociedad Contractual Minera Carola, Sociedad Punta del Cobre S.A., for access and support during field work, and their geologists for valuable information and discussion. Logistic support from the Instituto de Geología Económica Aplicada, Universidad de Concepción and Hanns Sylvester, Universidad de Atacama, Copiapó is gratefully acknowledged. François Bussy, Mercè Ferrés, Todd Feeley, and Osman Parlak are also thanked for their analytical assistance. Early drafts of this manuscript benefitted from critical comments by Jeffrey Hedenquist, Christoph Heinrich, Michael Dungan, and Theresa Boundy. Formal reviews by Simon Kelley and Finlay Stuart helped us to clarify many points and are greatly appreciated. Support by Swiss National Science Foundation (SNSF) grants 2000-040575.94 and 2000-047269.96, Proyecto FONDECYT 1033-89, and the Deutsche Akademische Austauschdienst (DAAD) is gratefully acknowledged. The University of Geneva $^{40}Ar/^{39}Ar$ Geochronology Laboratory was constructed in part with funds from SNSF grant 21-31449.93.

Appendix

Complete $^{40}Ar/^{39}Ar$ incremental-heating data from two samples

Temperature °C	$^{40}Ar/^{39}Ar$	$^{37}Ar/^{39}Ar$[a]	$^{36}Ar/^{39}Ar$	$^{40}Ar^{*}$ (10^{-13} mol)	% $^{40}Ar^{*}$	K/Ca	^{39}Ar cumulative %	Apparent age ± 2σ Ma[b]
PC 938	biotite	0.45 mg	J = 0.003856 ± 0.000012			Total gas age = 114.1 ± 1.0 Ma		
700	8.703	0.241	0.04841	0.68	37.84	2.03	0.7	59.54 ± 5.14
800	15.907	0.208	0.03109	4.92	63.41	2.35	3.6	107.39 ± 3.76
850[c]	17.000	0.174	0.02459	15.78	70.08	2.82	12.1	*114.54 ± 2.05*
875	17.006	0.120	0.00568	12.48	91.04	4.08	18.8	*114.58 ± 1.94*
900	16.967	0.131	0.01098	9.07	83.97	3.74	23.7	*114.33 ± 1.43*
925	16.917	0.166	0.00980	5.70	85.42	2.95	26.8	*114.00 ± 1.68*
975	16.962	0.213	0.01109	10.28	83.56	2.30	32.4	*114.29 ± 2.22*
1025	16.947	0.170	0.00676	18.19	89.49	2.89	42.2	*114.19 ± 2.53*
1075	17.124	0.158	0.00499	34.20	92.11	3.09	60.6	*115.35 ± 1.93*
1125	17.076	0.154	0.00537	34.66	91.53	3.17	79.2	*115.04 ± 1.50*
1150	17.026	0.118	0.00425	18.98	93.15	4.15	89.4	*114.71 ± 1.74*
1175	17.030	0.120	0.00364	16.63	94.08	4.07	98.4	*114.74 ± 1.54*
1225	17.064	0.449	0.02663	2.21	68.52	1.09	99.6	*114.96 ± 3.04*
1300	16.349	2.380	0.06969	0.78	44.44	0.21	100.0	*110.29 ± 8.24*
PC 1027	whole-rock	0.25 mg	J = 0.003827 ± 0.000011			Total gas age = 90.1 ± 0.6 Ma		
650	13.771	0.006	0.00767	2.65	84.91	88.40	2.4	86.08 ± 1.59
750	13.054	0.004	0.00199	11.03	84.66	125.83	12.2	87.94 ± 0.84
800[c]	13.120	0.008	0.13115	11.01	77.18	60.25	21.2	*88.38 ± 1.26*
825[c]	13.134	0.004	0.01350	7.49	76.69	110.63	27.8	*88.47 ± 0.85*
850	13.052	0.005	0.00647	5.38	87.20	105.49	32.6	*87.93 ± 1.18*
900	13.269	0.003	0.00555	9.69	88.97	125.41	41.0	*89.36 ± 0.76*
940	13.351	0.004	0.00555	11.64	89.04	117.30	51.1	*89.89 ± 0.62*
970	13.420	0.004	0.01275	8.94	78.06	121.76	58.9	*90.35 ± 0.72*
1000	13.383	0.006	0.00836	7.68	84.40	79.00	65.5	90.11 ± 0.94
1040	13.515	0.007	0.01058	6.41	81.20	71.13	71.0	90.98 ± 0.96
1120	13.462	0.007	0.01287	8.74	77.96	67.10	78.5	90.62 ± 1.20
1250	13.722	0.005	0.00653	16.48	87.64	108.83	92.5	92.33 ± 0.68
1400	14.032	0.008	0.00731	9.12	86.64	58.01	100.0	94.36 ± 0.91

[a] Corrected for ^{37}Ar and ^{39}Ar decay, half-lives of 35 days and 259 years, respectively
[b] Ages calculated relative to HDB-1 biotite (24.292 Ma; Wijbrans et al. 1995; see text), ±2σ errors. $\lambda_E = 0.581 \times 10^{-10}$/y; $\lambda_B = 4.692 \times 10^{-10}$/y
[c] Temperature and age of plateau steps are in italics

References

Aguirre L, Levi B, Offler R (1978) Unconformities as mineralogical breaks in the burial metamorphism of the Andes. Contrib Mineral Petrol 66: 361–366

Arévalo C (1994) Mapa Geológico de la Hoja Los Loros. SERNAGEOMIN, Documentos de Trabajo 6

Arévalo C (1995) Mapa Geológico de la Hoja Copiapó (1: 100.000): Región de Atacama. SERNAGEOMIN, Documentos de Trabajo 8

Bookstrom AA (1977) The magnetite deposit of El Romeral, Chile. Econ Geol 72: 1101–1130

Brannon JC, Podesk FA, McLimans RK (1992) A Permian Rb-Sr age for sphalerite from the Upper Mississippi Valley lead-zinc district, Wisconsin. Nature 356: 509–511

Brown PE, Hagemann SG (1995) Fluid inclusion data reduction and interpretation using MacFlinCor on the Macintosh. Bol Soc Española Mineral 18-1: 32–33

Camus F (1980) Posible modelo genético para los yacimientos de cobre del distrito minero Punta del Cobre. Rev Geol Chile 11: 51–76

Camus F (1986) Los yacimientos estratoligados de Cu, Pb-Zn y Ag de Chile. In: Frutos J, Oyarzún R, Pincheira M (eds) Geología y recursos minerales de Chile. Editorial Univ. de Concepción, Concepción, vol 2, pp 547–635

Cathelineau M, Nieva D (1985) A chlorite solid solution geothermometer: the Los Azufres (Mexico) geothermal system. Contrib Mineral Petrol 91: 235–244

Cebula GT, Kunk MJ, Mehnert HH, Naeser CW, Obradovich JD, Sutter JF (1986) The Fish Canyon Tuff, a potential standard for the $^{40}Ar/^{39}Ar$ and fission track methods (abst.). Terra Cognita 6: 139–140

Chesley JT, Halliday AN, Kyser TK, Spry PG (1994) Direct dating of Mississippi Valley-type mineralization: use of Sm-Nd in fluorite. Econ Geol 89: 1192–1199

Corvalán J (1974) Estratigrafia del Neocomiano marino de la región al sur de Copiapó, Provincia de Atacama. Rev Geol Chile 1: 13–36

Cowie JW, Bassett MG (1989) International Union of Geological Sciences. 1989 Global Stratigraphic Chart. Episodes 12, supplement

Dalrymple GB (1979) Critical tables for conversion of K-Ar ages from old to new constants. Geology 7: 558–560

Deino A, Potts R (1990) Single-crystal $^{40}Ar/^{39}Ar$ dating of the Olorgesailie formation, southern Kenya Rift. J Geophys Res 95: 8453–8470

Espinoza S (1990) The Atacama-Coquimbo ferriferous belt, northern Chile. In: Fontboté L, Amstutz GC, Cardozo M,

Cedillo E, Frutos J (eds) Stratabound ore deposits in the Andes. Springer, Berlin Heidelberg New York, pp 353–364
Farrar E, Clark AH, Haynes SJ, Quirt GS, Conn H, Zentilli M (1970) K-Ar evidence for the post-Paleozoic migration of granitic intrusion foci in the Andes of northern Chile. Earth Planet Sci Lett 10: 60–66
Friedman I, O'Neil JR (1977) Compilation of stable isotope fractionation factors of geochemical interest. In: Fleischer M (ed) Data of geochemistry. US Geol Surv Prof Pap 440-KK, 12 p
Harland WB, Armstrong RL, Cox AV, Craig LE, Smith AG, Smith DG (1990) A geologic time scale 1989. Cambridge University Press, 263 p
Hey MH (1954) A new review of the chlorites. Mineral Mag 30: 277–292
Hopf S (1990) The Agustina Mine, a volcanic-hosted copper deposit in northern Chile. In: Fontboté L, Amstutz GC, Cardozo M, Cedillo E, Frutos J (eds) Stratabound ore deposits in the Andes. Springer, Berlin Heidelberg New York, pp 421–434
Jurgan H (1977) Strukturelle und lithofazielle Entwicklung des andinen Unterkreide-Beckens im Norden Chiles (Provinz Atacama). Geotekt Forsch 52, 138 p
Levi B (1970) Burial metamorphic episodes in the Andean geosyncline, Central Chile. Geol Rundsch 59: 994–1013
Lino S (1984) Geología de la mina Agustina, Comuna de Tierra Amarilla, Provincia de Copiapó, Region de Atacama. Unpublished Memoria de Titulo, Universidad Catolica del Norte, Antofagasta, 161 p
Lippolt HJ, Hess J (1994) Compilation of K-Ar measurements on HD-B1 standard biotite 1994 status report. In: Odin GS (ed) Phanerozoic time scale. IUGS Subcom Geochronol 12: 18–23
Marschik R, Schönfelder H, Fontboté L (1993) Alteration trends in the Punta del Cobre mining district, North Chile: a preliminary study (Abstr). Low Temperature Metamorphism: Processes, Products and Economic Significance, Symp IGCP Project 294, Santiago, 1993, pp 57–64
Marschik R, Fontboté L (1994) Potassium and sodium alteration related to Cu-mineralization in the Punta del Cobre Formation, northern Chile. Congr Geol Chileno, 7th, Concepción, 1994, Actas, vol 2, pp 1591–1595
Marschik R, Fontboté L (1995) Superposed alteration and volcanic-hosted Cu(-Fe) mineralization in the Punta del Cobre belt, northern Chile: a new type of intrusion related deposit? In: Pasava J, Kríbek B, Zák K (eds) Mineral deposits: from their origin to their environmental impacts. Balkema, Rotterdam, pp 477–481
Marschik R Fontboté L (1996) Copper(-iron) mineralization and superposition of alteration events at the Punta del Cobre Belt, northern Chile. In: Camus F, Sillitoe RH, Petersen R, Sheahan P (eds) Andean copper deposits: New discoveries, mineralization, styles and metallogeny. Econ Geol Spec Publ 5: 171–189
Marschik R, Chiaradia M, Fontboté L (1997) Intrusion-related Cu(-Fe)-Au mineralization in the Punta del Cobre belt, Chile: lead and sulfur isotopic constraints: Balkema, Rotterdam
McDougall I, Harrison TM (1988) Geochronology and thermochronology by the $^{40}Ar/^{39}Ar$ method. Oxford University Press, 212 p
Ménard JJ (1992) Comparaison entre les roches plutoniques associées à la ceinture de fer du Chili et aux porphyres cuprifères: arguments pétrologiques. Compt Rend Acad Sci, Paris, 315: 725–731
Ménard JJ (1995) Relationship between altered pyroxene diorite and the magnetite mineralization in the Chilean Iron Belt, with emphasis on the El Algarrobo iron deposits (Atacama region, Chile). Mineralium Deposita 30: 268–274
Mortimer C (1973) The Cenozoic history of the southern Atacama Desert, Chile. J Geol Soc London 129:505–526
Munizaga F, Huete C, Hervé F (1985) Geochronología K-Ar y razones iniciales $^{87}Sr/^{86}Sr$ de la "Faja Pacífica" de "Desarollos Hidrothermales". Congr Geol Chileno, 4th, Antofagasta, 1985, Actas, vol 3, pp 357–379
Nakei S, Halliday AN, Kesler SE, Jones HD, Kyle RJ, Lane TE (1993) Rb-Sr dating of sphalerite from Mississippi Valley-type ore deposits. Geochim et Cosmochim Acta 57: 417–427
Nisterenko GV, Losert J, Chavez L, Naumov VB (1973) Temperaturas y presiones de formación alunos yacimientos cupríferos de Chile. Rev Geol Chile 1: 74–84
Nysten P (1986) Gold in the volcanogenic mercury-rich sulfide deposit Långsele, Skellefte ore district, northern Sweden. Mineralium Deposita 21: 116–120
Palacios CM (1990) Geology of the Buena Esperanza copper-silver deposit, northern Chile. In: Fontboté L, Amstutz GC, Cardozo M, Cedillo E, Frutos J (eds) Stratabound ore deposits in the Andes. Springer, Berlin Heidelberg New York, pp 313–318
Perkins C (1996) $^{40}Ar/^{39}Ar$ age constraints on deformation and mineralization, Rosebery Zn-Pb-Cu and Mount Lyell Cu deposits, Tasmania, Australia. Mineralium Deposita 31: 71–83
Pincheira M (1985) Reseña de las características geológicas de los principales yacimientos de hierro del Norte de Chile. In: Frutos J, Oyarzún R, Pincheira M (eds) Geología y recursos minerales de Chile. Editorial Univ. de Concepción, Concepción, vol 2, pp 717–737
Pincheira M (1991) Mn-Fe-Mantos in "intra-arc" Becken des unterkretazischen magmatischen Bogens Nordchile (Küstenkordillere, 27°–29 °S): Tektonischer Rahmen, Petrographie und Geochemie von Erz und Nebengestein. Heidelb Geowiss Abh 46, 304 p
Potter RW II, Babcock RS, Brown DL (1977) A new method for determining the solubility of salts in aqueous solutions at elevated temperatures. J Res US Geol Surv 5: 389–395
Rabbia OM, Frutos J, Pop N, Isache C, Sanhueza V, Edelstein O (1996) Características isotópicas de la mineralización de Cu(-Fe) de Mina Carola, distrito minero Punta del Cobre, norte de Chile. Congr Geol Argentino, 8th, Buenos Aires, 1996, Actas, vol 3: 241–254
Roedder E (1984) Fluid inclusions. Mineral Soc America, Reviews in Mineralogy 12, 644 p
Ryan PJ, Lawrence AI, Jenkins RA, Matthews JP, Zamora JC, Marino E (1994) The Candelaria copper-gold deposit, Chile. Congr Geol Chileno, 7th, Concepción, 1994, Actas, 2: 1616–1617
Ryan PJ, Lawrence AI, Jenkins RA, Matthews JP, Zamora JC, Marino E, Urqueta I (1995) The Candelaria copper-gold deposit, Chile. In: Pierce FW, Bolm JG (eds) Porphyry copper deposits of the American Cordillera. Arizona Geol Soc Digest 20: 625–645
Sato T (1984) Manto type copper deposits in Chile – a review. Bull Geol Surv Japan 35: 565–582
Segerstrom K (1967) Geology and ore deposits the central Atacama Province, Chile. Geol Soc Am Bull 78: 305–318
Segerstrom K, Parker RL (1959) Cuadrángulo Cerrillos, Provincia de Atacama. Santiago, Inst Invest Geol, Carta Geol Chile, vol 1 (2) 33 p
Segerstrom K, Ruiz C (1962) Geología del Cuadrángulo Copiapó, Provincia de Atacama. Santiago, Inst Invest Geol, Carta Geol Chile, vol 3 (1) 115 p
Sillitoe RH (1988) Epochs of intrusion-related copper mineralization in the Andes, J South Am Earth Sci 1: 89–108
Sillitoe RH, Mortimer C, Clark AH (1968) A chronology of landform evolution and supergene mineral alteration, southern Atacama Desert, Chile. Trans Inst Min Metall 77B: 166–169
Singer BS, Pringle MS (1996) Age and duration of the Matuyama-Brunhes geomagnetic polarity reversal from $^{40}Ar/^{39}Ar$ incremental-heating analyses of lavas. Earth Planet Sci Lett 139: 47–61
Snee LW, Sutter JF, Kelly WC (1988) Thermochronology of economic mineral deposits: Dating the stages of mineralization at Panasquiera, Portugal, by high-precision $^{40}Ar/^{39}Ar$ age spectrum techniques on muscovite. Econ Geol 83: 335–354
Steiger RH, Jäger E (1977) Subcommision on geochronology: convention on the use of decay constants in geo- and cosmochronology. Earth Planet Sci Lett 36: 359–362

Sterner SM, Bodnar RJ (1984) Synthetic fluid inclusions in natural quartz. I. Compositional types synthesized and applications to experimental geochemistry. Geochim Cosmochim Acta 48: 2659–2668

Sutter JF, Hartung JB, Kelly WC (1983) Laser probe $^{40}Ar/^{39}Ar$ dating of individual grains from the tin-tungsten mineralization at Panasqueira, Portugal. GSA Abstr 15: 702

Tilling R (1962) Batholith emplacement and contact metamorphism in the Paipote-Tierra Amarilla area, Atacama Province, Chile. Unpublished PhD Thesis, Yale University, Newhaven, Connecticut, 195 p

Tilling R (1963a) Batholith emplacement and contact metamorphism near Tierra Amarilla, Atacama Province, Chile (Abstr). Geol Soc Am Spec Pap 76: 166–167

Tilling R (1963b) Disequilibrium skarns of the Tierra Amarilla aureole, Atacama province, Chile (Abstr). Geol Soc Am Spec Pap 76: 167

Tilling R (1976) El Batholito Andino cerca de Copiapó, Provincia de Atacama. Geología y Petrología. Rev Geol Chile 3: 1–24

Wijbrans JR, Pringle MS, Koppers AAP, Schevers R (1995) Argon geochronology of small samples using the Vulkaan argon laserprobe. Proc Kon Ned Akad Wet 98: 185–218

Williams-Jones AE, Samson IM (1990) Theoretical estimation of halite solubility in the system NaCl-$CaCl_2$-H_2O: application to fluid inclusions. Can Mineral 28: 299–304

Wolf F, Fontboté L, Amstutz GC (1990) The Susana copper (-silver) deposit in northern Chile, hydrothermal mineralization associated with a Jurassic volcanic arc. In: Fontboté L, Amstutz GC, Cardozo M, Cedillo E, Frutos J (eds) Stratabound ore deposits in the Andes. Springer, Berlin Heidelberg New York, pp 319–338

Woods TL, Bethke PM, Bodnar RJ, Werre RW Jr (1981) Supplementary components and operation of the US Geological Survey gas-flow heating/freezing stage. US Geol Surv Open File Rep pp 81–954

York D (1966) Least-squares fitting of a straight line. Can J Phys 44: 1079–1086

York D, Masliwec A, Kuybida P, Hanes JA, Hall CM, Kenyon WJ, Spooner ETC, Scott SD (1981) $^{40}Ar/^{39}Ar$ dating of pyrite. Nature 300: 52–53

Zentilli M (1974) Geological evolution and metallogenetic relationships in the Andes of northern Chile between 26 ° and 29 ° S. Unpublished PhD Thesis, Queen's University, Kingston, Ontario, Canada, 394 p